TECHNICAL TRANSACTIONS | **CZASOPISMO TECHNICZNE**
CHEMISTRY | CHEMIA
2-Ch/2014

GIUSEPPINA MONTANTE*, MIRELLA CORONEO*, FRANCO MAGELLI*,
ALESSANDRO PAGLIANTI*

PREDICTION OF TURBULENT FLUID MIXING IN CORRUGATED STATIC MIXERS

PRZEWIDYWANIE BURZLIWEGO MIESZANIA W POFALOWANYCH MIESZALNIKACH STATYCZNYCH

Abstract

This work deals with the analysis of the turbulent flow of Newtonian fluids in pipelines equipped with corrugated plate static mixers. The investigation is carried out by Computational Fluid Dynamics simulations based on the numerical solution of the Reynolds Averaged continuity, momentum and scalar transport equations coupled with the standard k–ε turbulence model. The mixing characteristics of the SMV mixer in blending two miscible liquids having equal or different density are presented and the effects of different operating conditions are discussed. Finally, the effectiveness of the simulation results to provide guidelines for the optimization of the static mixing operating conditions and design are highlighted.

Keywords: *mixer*, *SMV*, *turbulent flow*, *blending*, *Computational Fluid Dynamics*

Streszczenie

Niniejszy artykuł poświęcony jest analizie burzliwego przepływu płynów newtonowskich przez przewód wyposażony w mieszalniki statyczne z pofalowanych płyt. Badania przeprowadzono, wykorzystując symulacje CFD oparte na numerycznym rozwiązaniu uśrednionych metodą Reynoldsa równań ciągłości, pędu i skalarnych równań przenoszenia, połączonych ze standardowym modelem burzliwości k–ε. Charakterystyki mieszania mieszalnika statycznego SMV w procesie mieszania dwóch wzajemnie się mieszających cieczy mających taką samą lub różną gęstość omówiono również wpływ różnych parametrów ruchowych. Na zakończenie przedstawiono efektywność wyników symulacji i ich znaczenie w optymalizacji warunków pracy mieszalników statycznych

Słowa kluczowe: mieszalnik statyczny, SMV, przepływ burzliwy, mieszanie, CFD

* Prof. Giuseppina Montante, Prof. Franco Magelli, CHIMIND, Ph.D. Mirella Coroneo, Prof. Alessandro Paglianti, DICAM, Università di Bologna, Italy.

1. Introduction

Static mixers are often adopted as an alternative to the most widespread dynamic agitators in a variety of industrial applications for in-line blending of liquids, liquid-liquid emulsions or gas-liquid dispersions. A number of different static mixing elements have been developed so far; the design selection for each application depends mainly on the specific single- or multi- phase fluids to mix and on the flow regime of the process. Similarly to the mechanical agitators, due to the complex fluid dynamic characteristics of any mixing devise, general design rules for static mixers have not been devised (Paglianti and Montante, 2013). Overall, extensive data and correlations are available on pressure drops at least for the most widespread static mixers (Thakur et al., 2003), while the flow features and the mixing mechanisms have been investigated in a limited number of works (Marshall and Bakker, 2004). Computational Fluid Dynamics (CFD) simulations are virtually able to provide detailed information on the flow features and on the mixing effectiveness of static mixers and they are increasingly adopted for the design, the optimization and the selection of operating conditions. This investigation is focused on the analysis of the corrugated plate static mixers, which are widely adopted in industry particularly for turbulent flows and limited mixing length applications (Etchells and Meyer, 2004). With respect to other widespread static mixers, SMVs have been less investigated by either experimental and numerical methods. On the computational side, recently the capability of a Reynolds Averaged Navier-Stokes (RANS) simulation method in accurately describing the main fluid dynamic characteristics of corrugated plate mixers has been assessed trough comparison with literature velocity and tracer concentration data by Coroneo et al. (2012). The model equations and the solution methods, which were shown to minimize the numerical errors and to provide reliable results, are adopted in this work in order to analyze the mixing performances and the pressure drops of a pipeline equipped with a SMV element, in which the blending two miscible liquids of equal or different density is accomplished at various flow rates of the two streams.

2. The Model Equations

The simulations were based on the solution of the conservation equations of mass, momentum and scalar concentration for incompressible, isothermal and steady-state flow of Newtonian liquids. Since the flow regime was fully turbulent for all the investigated conditions, the Reynolds-Averaged formulation was adopted. The resulting equations are as follows:

$$\nabla \cdot (\rho \mathbf{U}) = 0 \tag{1}$$

$$\nabla \cdot (\rho \mathbf{U}\mathbf{U}) = -\nabla p + \mu \nabla^2 \mathbf{U} - \nabla \cdot (\rho \overline{\mathbf{u}'\mathbf{u}'}) + \rho g \tag{2}$$

$$\nabla \cdot (\rho \mathbf{U} \Phi_i) = \nabla \cdot \left(\rho D_m \nabla \Phi_i + \frac{\mu_t}{\sigma_t} \nabla \Phi_i \right) \tag{3}$$

where:

U – is the mean velocity vector,

ρ – is the volume averaged density of the fluids,

g – is the gravity acceleration vector,
m – is the viscosity of the fluids,
p – is the pressure,
$\rho\overline{\mathbf{u}'\mathbf{u}'}$ – is the Reynolds stess tensor
F – is the volumetric fraction of the i liquid component,
m_t – is the turbulent viscosity,
s_t – is the turbulent Schmidt number,
D_m – is the molecular diffusion coefficient.

The molecular diffusion coefficient was fixed to the value of 10^{-9} m^2/s, though for fully turbulent flow regimes the overall tracer dispersion is dominated by the turbulent diffusion and the value of D_m is expected to be negligible. The turbulent diffusion coefficient depends on the ratio between the turbulent viscosity, which results from the turbulence closure equations, and the turbulent Schmidt number, that was fixed equal to 0.7, as is commonly suggested (Hartmann et al., 2006).

In this work, based on previous results (Coroneo et al., 2012), the Reynolds stress tensor was modelled using the eddy viscosity hypothesis. In particular, the RANS equations were closed with the following standard k–ε model equations:

$$\nabla\cdot\left(\rho\mathbf{U}k-\left(\mu+\frac{\mu_t}{\mu_k}\right)\nabla k\right)=G_k+G_b \tag{4}$$

$$\nabla\cdot\left(\rho\mathbf{U}\varepsilon-\left(\mu+\frac{\mu_t}{\sigma_\varepsilon}\right)\nabla\varepsilon\right)=(C_1G_k+C_3G_b-C_2\rho_c\varepsilon)\frac{\varepsilon}{k} \tag{5}$$

$$\mu_t=C_\mu\frac{k^2}{\varepsilon} \tag{6}$$

$$C_3=\mathbf{tanh}\left|\frac{u_x}{u_z}\right| \tag{7}$$

where:

k – is the turbulent kinetic energy,
e – is the dissipation of turbulent kinetic energy,
C_μ, C_1, C_2, s_k, s_ε, – are the standard k–ε model constant,
G_k – is the k production due to the mean velocity gradient,
G_b – is the k production due to buoyancy,
u_x – is the velocity component parallel to g,
u_y – is the velocity component perpendicular to g.

G_b is nil for equal density of the miscible liquids, while in case of different densities, it is calculated as follows:

$$G_b=-g\frac{\mu_t}{\rho\sigma_t}\nabla\rho \tag{8}$$

The viscosity-affected regions between the walls and the fully-turbulent regions were bridged by the standard wall functions proposed by Launder and Spalding (1974).

3. The Computational Domain and the Numerical Details

The computational domain, whose geometrical features are depicted in Figure 1, consists of an horizontal pipeline of diameter D equal to 50 mm and length equal to $10 \times D$ containing one static mixer element of standard length ($L = D$) and a coaxial tube of internal diameter equal to 10 mm. The SMV element consists of 5 corrugated plates 2 mm thick, forming channels inclined of 45° with respect to the pipeline main axis. The mixer inlet section is positioned at 3D from the main tube inlet section and at 20 mm from the secondary tube exit surface. The same geometry was already investigated in previous works by LDA and PLIF experiments (Karoui et al., 1997; 1998) and by CFD simulations (Coroneo et al., 2012). Therefore, the numerical solution of the model equations adopted in this work is based on the conclusions gained from the comparison of the simulation results of Coroneo et al. (2012) with the experimental data collected by Karoui et al. (1997, 1998)

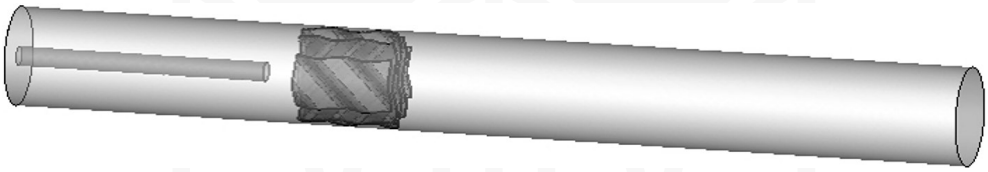

Fig. 1. The geometrical characteristics of the computational domain

The domain discretization was performed by an unstructured grid consisting of 4.4×10^6 cells. The model equations were numerically solved by adopting the finite volume CFD code FLUENT 6.3. The conservation equations were integrated in space using a second order upwind discretization scheme for the convective terms. The SIMPLEC algorithm was used to couple pressure and velocity. As for the boundary conditions, at the walls of the static mixer insert and of the pipelines no-slip boundary conditions were imposed, at the two fluid flow entrances velocity inlet boundary condition were selected and at the domain outlet boundary a pressure of 1.01×10^5 Pa was set.

The solution convergence was checked by monitoring the residuals of all the variables, the mass balance and the concentration of the scalars at the outlet section. At the end of the calculations, most of the variables residuals were dropped to the order of 10^{-6}.

The model equation were written with respect to a fixed Cartesian coordinate system, namely: x, y, z. The pipeline axis was placed along the z direction, while the gravity vector acted along the negative x direction. The origin was placed on the centre of the upstream surface of the static mixer element.

4. The flow conditions

Four simulation cases, listed in Table 1, were considered in order to investigate the effect of the liquid density and of the flow rate of the two streams on the mixing performances obtained in the pipeline. In the following, the subscript L and S will be adopted for the variables relevant to the larger and the smaller pipe, respectively.

Table 1

Main parameters of the simulated conditions

	ρ_S/ρ_L [–]	$V_{inlet,L}$ [m/s]	$V_{inlet,S}$ [m/s]	Q_S/Q_L [–]	$Re_L \times 10^4$ [–]	$Re_S \times 10^4$ [–]	Fr' [–]
Case A	1	0.62	29.85	1.91	3.02E+00	28.94	101.9
Case B	1.25	0.62	29.85	1.91	3.02E+00	36.23	118.7
Case C	1.25	0.31	14.93	1.91	1.51E+00	18.11	29.7
Case D	1.25	0.62	7.46	0.48	3.02E+00	9.05	28.4

The reference operating condition (Case A) was coincident with one of those discussed by Coroneo et al., that is the blending of a water stream fed at the flow rate of 4.75 m^3/h to the main pipe with a Rhodamine solution entering trough the smaller pipe at the flow rates of 8.05 m^3/h; under this conditions, the inlet velocity of the Rhodamine solution, $V_{inlet,S}$, is 48 times the water superficial velocity, $V_{inlet,L}$, and the density ratio of the two liquids, r_S/ρ_L, is equal to 1.

A different density of the two liquids was considered in the other cases. In particular, the density of the stream fed to the larger pipe was kept constant, while for the smaller pipe stream, the density of a solution of sodium hypochlorite at 15 vol. % in water was set, which is 1.25 times bigger than the water density. In order to consider the effect of the density difference only, in Case B the same flow rates of case A were considered. Instead, the fluid flow variations were considered in case C and D. In the former case, the flow rates of both the streams have been halved, thus resulting in the same flow rate ratio, Q_S/Q_L, but to halved Reynolds numbers; in the latter case the flow rate of the smaller pipe stream was reduced to one fourth with respect to the reference Case A. The Reynolds numbers reported in Table 1 have been calculated with reference to the inlet pipe sections, while the densiometric Froude number (Streiff et al, 1999), Fr′, is defined as:

$$\mathrm{Fr}' = \frac{\rho V_m^2}{(\rho_S - \rho_L) g D_H} \tag{9}$$

where:

V_m – is the mean superficial velocity,
D_H – is the mixer hydraulic diameter.

5. Results and discussion

The main features of the liquid homogenization for the four cases listed in Table 1 are firstly analysed by a comparison of the colour maps of the liquid volumetric fraction on selected planes. Since just two liquids are involved, the feed to the smaller tube only is considered. The results obtained in the vertical and horizontal planes passing trough the tube axis are shown in Figure 2 and 3, respectively. As can be observed from the comparison of the maps relevant to Case A and Case B, the effect of the different density ratio can be appreciated clearly upstream the SMV element, where a different degree of backmixing is apparent. Slight differences are obtained also up to 3D downstream the mixer, thus confirming that for densiometric Froude number higher than 20, as in the cases considered in this work (Table 1), the density difference does not produce significant effects (Streiff et al., 1999). As for the fluid dynamic conditions, halving the flow rates (Case C) apparently does not give rise to any appreciable concentration variation, while a significantly different result is obtained for the lowest flow rate in the smaller tube (Case D) either upstream and downstream the SVM.

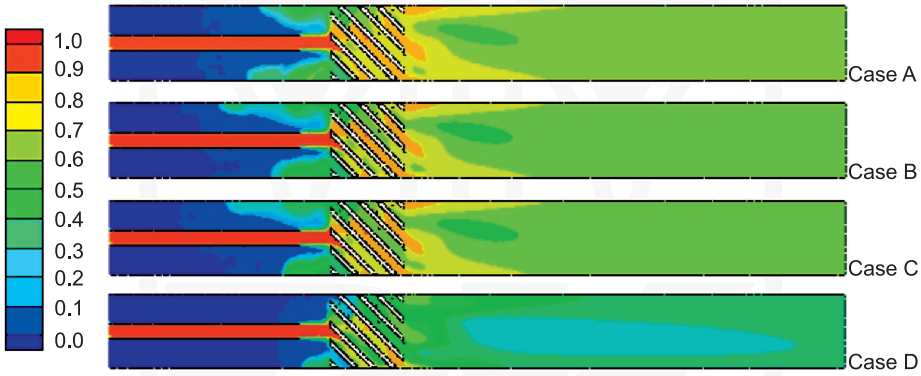

Fig. 2. Volume fraction of the liquid entering from the smaller tube on a diametrical vertical plane

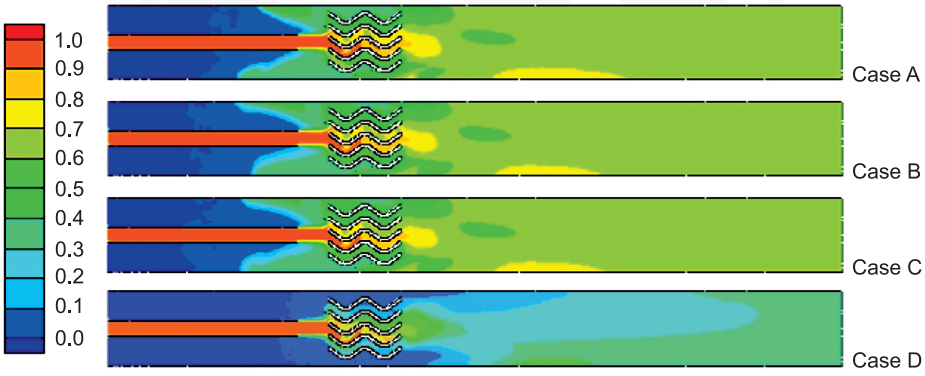

Fig. 3. Volume fraction of the liquid entering from the smaller tube on a diametrical horizontal plane

The degree of liquid mixing inside the SVM in the different cases can be qualitatively evaluated observing the liquid concentration at the mixer inlet ($z = 0$) and outlet ($z = D$) cross sections, shown in Figures 4 and 5. As far as a coaxial distributor is adopted, as in the present geometry, the concentration distribution exhibits higher values in the central tube

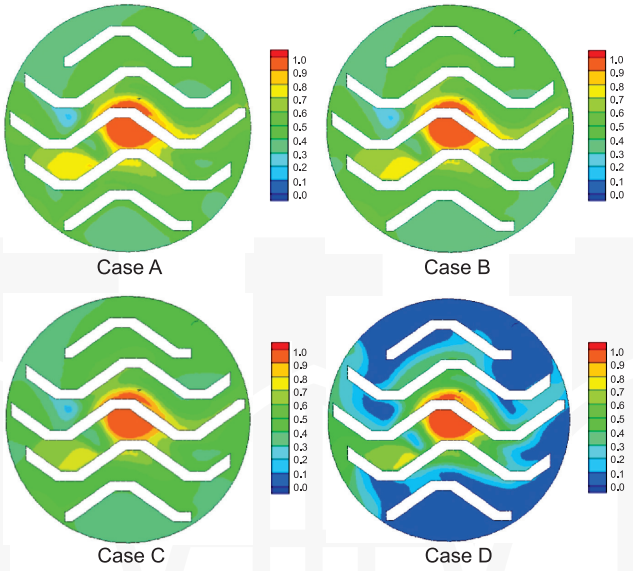

Fig. 4. Volume fraction of the liquid entering from the smaller tube on the mixer inlet cross section

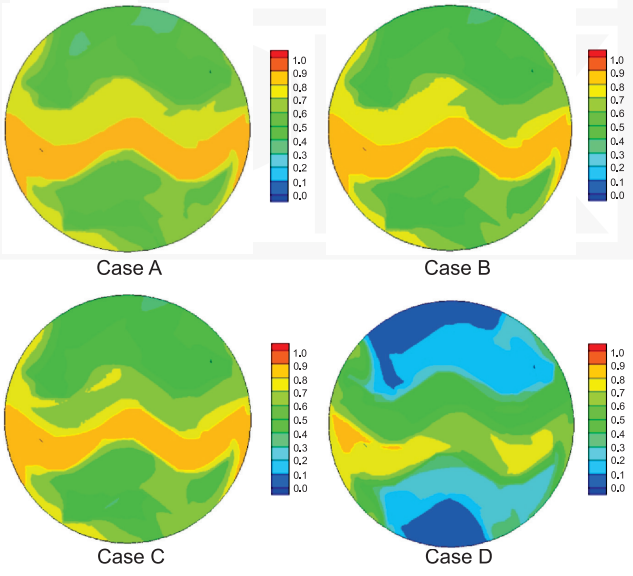

Fig. 5. Volume fraction of the liquid entering from the smaller tube on the mixer outlet cross section

region also at the mixer exit, although a distribution along the whole horizontal section takes place. Improved performances can be expected by an optimized distributor design (Etchells and Meyer, 2004; Coroneo et al., 2011). Overall, the concentration differences due to the density variation and the flow characteristics already observed in the diametrical planes are confirmed also in the pipelines cross sections.

The coefficient of variation (CoV) is also adopted for assessing the static mixer performance in the different conditions, adopting the following definitions:

$$\mathrm{CoV} = \sqrt{\frac{\sum_{i=1}^{N}(c_i - c_{\mathrm{mean}})^2}{N-1}}\,\frac{1}{c_{\mathrm{mean}}} \tag{10}$$

where:

c_i – is the local concentration at the i-th evaluation point,
c_{mean} – is the calculated mean concentration of the additive on the cross section,
N – is number of evaluation positions at the actual cross section.

The evaluation position corresponds to each grid cell in the considered section. The pipeline length for achieving the well mixed condition is identified by the often adopted CoV value of 0.05.

The CoV values along the pipe axial coordinate shown in Figure 6 for the reference condition (Case A) show that the well mixed condition is achieved after 2D from the SVM inlet section and that a significant degree of homogenization is obtained in the empty tube length of *D* just downstream the mixer element. The comparison of the CoV profiles obtained under the four different conditions shown in Figure 7 highlights that the density variation considered in this work does not affect the CoV value significantly, while the mixing performances are dominated from the flow rate ratio.

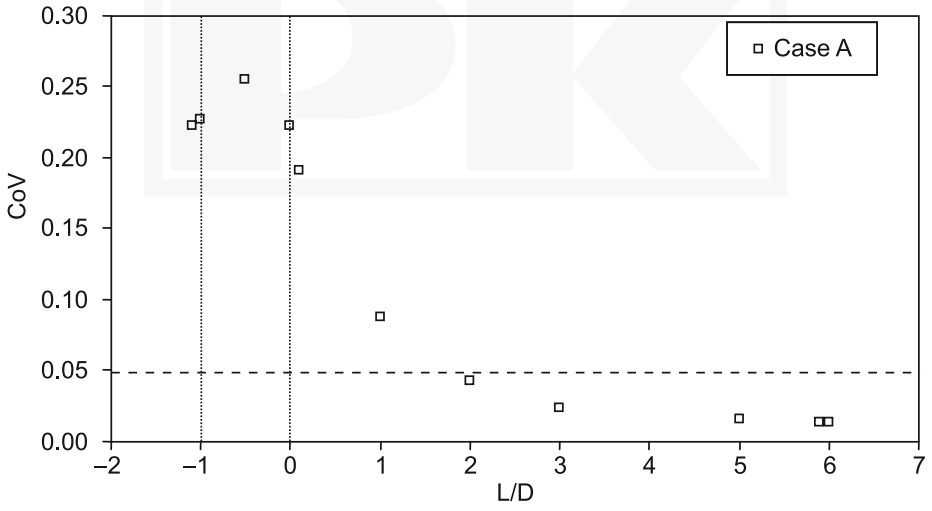

Fig. 6. CoV profile at different cross section of the pipeline

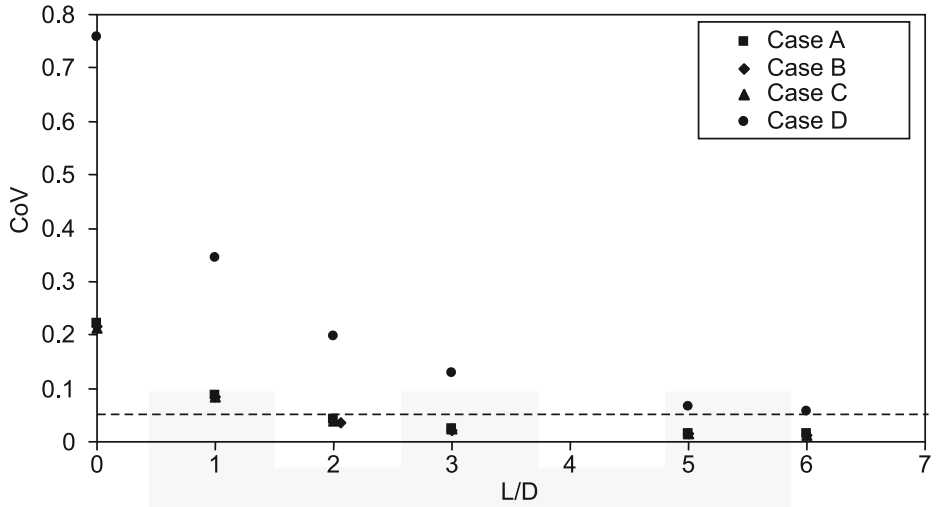

Fig. 7. Comparison of CoV profiles at different cross section of the pipeline

The capability of the present CFD simulation method to provide reliable estimate of the pressure drops is assessed by comparison with the prediction of the correlation recently proposed by Paglianti and Montante (2013) and the results are reported in Figure 8. As can be observed, a good accuracy is obtained, thus adding a further verification of the robustness the present approach for the design and the optimization of corrugated plate static mixers for turbulent flow applications. Further work has to be carried out for extending this conclusion to multiphase flow conditions.

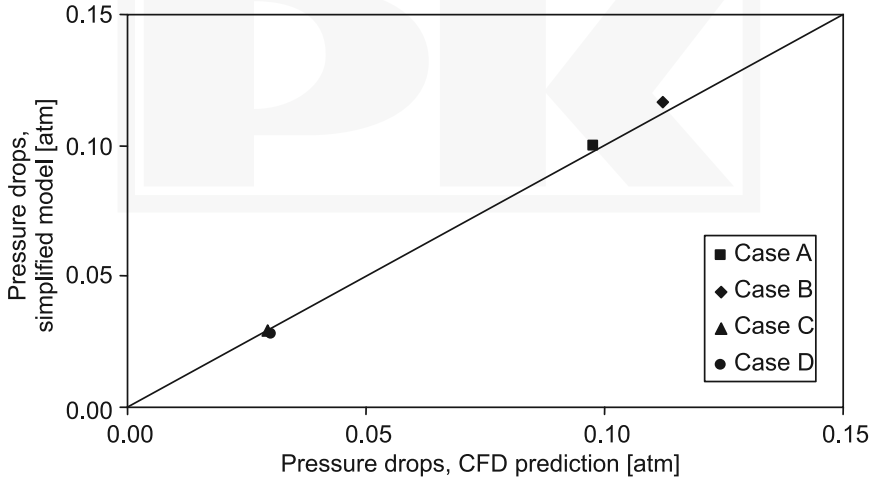

Fig. 8. Comparison of the DP predictions in the four simulated cases

References

[1] Coroneo M., Montante G., Paglianti A., *Computational fluid dynamics modeling of corrugated static mixers for turbulent applications*, Industrial and Engineering Chemistry Research, 51, 2012, 15986-15996.

[2] Etchells A.W., Meyer C.F., 2004. Chaper 7, *Mixing in Pipelines*, p. 422-424, [in:] Paul E.L., Atiemo-Obeng V.A., Kresta, S.M. (Eds.), *Handbook of Industrial Mixing*, Wiley-Interscience: Hoboken, NJ.

[3] Hartmann H., Derksen J.J., Van den Akker H.E.A., *Mixing times in a turbulent stirred tank by means of LES*, AIChE Journal, 52, 2006, 3696-3706.

[4] Karoui A., Hakenholz F., Le Sauze N., Costes J., Bertrand J., *Determination of the mixing performance of sulzer SMV static mixers by laser induced fluorescence*, Can. J. Chem. Eng., 76, 1998,522-526.

[5] Karoui A., Le Sauze N., Costes J., Bertrand J., *Experimental and numerical study of flow at the outlet of Sulzer SMV static mixers*, Récents Progrès en Génie des Procédés, 11, 1997, 323-330.

[6] Launder B.E., Spalding D.B., *The numerical computation of turbulent flows*, Comput. Meth. Appl. Mech. Engrg., 3, 1974, 269-289.

[7] Marshall E.M., Bakker A., 2004, Chapter 5, *Computational Fluid Mixing*, p. 325, [in:] Paul E.L., Atiemo-Obeng V.A., Kresta S.M. (Eds.), *Handbook of Industrial Mixing*, Wiley-Interscience: Hoboken, NJ.

[8] Paglianti A., Montante G., *A mechanistic model for pressure drops in corrugated plates static mixers*, Chemical Engineering Science, 97, 2013, 376-384.

[9] Streiff F.A., Jaffer S., Schneider G., 1999, *The design and application of static mixer technology*, Third International Symposium on Mixing in Industrial Processes, Osaka, Japan, September 19th–22th., 107-114.

[10] Thakur R.K., Vial Ch., Nigam K.D.P., Nauman E.B., Djelveh G., *Static Mixers in the process industries- A review*, Chemical Engineering Research and Design, 81, 2003, 787-826.